Journal of Biomechanics 44 (2011) 1478–1483

Contents lists available at ScienceDirect

Journal of Biomechanics

journal homepage: www.elsevier.com/locate/jbiomech
www.JBiomech.com

The feasibility of modal testing for measurement of the dynamic characteristics of goat vertebral motion segments

S.J.P.M. van Engelen [a,b], A.J. van der Veen [c], A. de Boer [d], M.H.M. Ellenbroek [d], T.H. Smit [a,e,f], B.J. van Royen [a,e,f], J.H. van Dieën [a,b,*]

[a] Research Institute MOVE, VU University Amsterdam, The Netherlands
[b] Faculty of Human Movement Sciences, VU University Amsterdam, The Netherlands
[c] Department of Physics and Medical Technology, VU University Medical Centre, Amsterdam, The Netherlands
[d] Department of Applied Mechanics, University of Twente, Enschede, The Netherlands
[e] Skeletal Tissue Engineering Group Amsterdam, VU University Medical Centre, Amsterdam, The Netherlands
[f] Department of Orthopaedic Surgery, VU University Medical Centre, Amsterdam, The Netherlands

ARTICLE INFO

Article history:
Accepted 9 March 2011

Keywords:
Biomechanics
Goat
Structural vibration testing
Resonance frequency
Mode shape

ABSTRACT

Structural vibration testing might be a promising method to study the mechanical properties of spinal motion segments as an alternative to imaging and spinal manipulation techniques. Structural vibration testing is a non-destructive measurement technique that measures the response of a system to an applied vibration as a function of frequency, and allows determination of modal parameters such as resonance frequencies (ratio between stiffness and mass), vibration modes (pattern of motion) and damping. The objective of this study was to determine if structural vibration testing can reveal the resonance frequencies that correspond to the mode shapes flexion–extension, lateroflexion and axial rotation of lumbar motion segments, and to establish whether resonance frequencies can discriminate specific structural alterations of the motion segment. Therefore, a shaker was used to vibrate the upper vertebra of 16 goat lumbar motion segments, while the response was obtained from accelerometers on the transverse and spinous processes and the anterior side of the upper vertebra. Measurements were performed in three conditions: intact, after dissection of the ligaments and after puncturing the annulus fibrosus. The results showed clear resonance peaks for flexion–extension, lateral bending and axial rotation for all segments. Dissection of the ligaments did not affect the resonance frequencies, but puncturing the annulus reduced the resonance frequency of axial rotation. These results indicate that vibration testing can be utilised to assess the modal parameters of lumbar motion segments, and might eventually be used to study the mechanical properties of spinal motion segments in vivo.

1. Introduction

Mechanical functioning of the spine is to a large extent determined by the mechanical properties of the intervertebral disc, facet joints and ligaments. Degeneration of the disc, facet joints and ligaments can lead to alterations in the stiffness of motion segments, which might cause the spine to become unstable (Schmidt et al., 1998; Haughton et al., 1999; Mao et al., 2005; Zhao et al., 2005). The stiffness of the spine may also be altered by spinal surgery. For example, surgery targeting spinal stenosis often implicates that the overlying lamina and the supraspinous ligament of the motion segment are removed, which might destabilise the spine (Tai et al., 2008; Subramaniam et al., 2009; Van Solinge et al., 2010).

The treatment of segmental instability aims at increasing segmental stiffness. To decide whether restabilising instrumentation is needed and which segments should be targeted, the exact location and severity of the instability need to be established. At present, the mechanical properties of individual spinal motion segments cannot be measured in vivo because MRI and X-ray images can only provide an estimate of the mechanical properties based on degeneration and instrumented spinal manipulation and intraoperative measurement devices can only obtain the mechanical properties of the entire spine; although these devices typically apply a transverse or bending force to the spinous processes and measure the deflection at the point of force application, they do not take into account that the load–displacement data of only one segment do not reflect the mechanical properties of this single segment, but of the tested as well as all adjacent segments.

* Corresponding author at: VU University, Faculty of Human Movement Sciences, Van der Boechorststraat 9, NL-1081 BT Amsterdam, The Netherlands.
E-mail addresses: j.h.van.dieen@vu.nl, j_h_van_dieen@fbw.vu.nl (J.H. van Dieën).

0021-9290
doi:10.1016/j.jbiomech.2011.03.013

An alternative method for measuring the mechanical properties of individual motion segments might be structural vibration testing, which measures the response of a system to an applied vibration as a function of frequency. The resulting frequency response function (FRF) allows determination of modal parameters such as resonance frequencies (ratio between stiffness and mass), vibration modes (pattern of motion) and damping. It is also possible to estimate the mass (m), stiffness (k) and damping (c) using a parameter estimation procedure based on the relationship between the FRF and the time domain differential equation of motion (see Eq. (1)), where $\dot{x}$ and $\ddot{x}$ are, respectively, the first and second derivative of displacement x, and $F(t)$ is the external force (Richardson, 1977):

$$m\ddot{x} + c\dot{x} + kx = F(t) \tag{1}$$

Vibration testing of the spine is not new, although previous vibration experiments were merely low frequency dynamic tests than modal tests. Kazarian (1972), Kaigle et al. (1998) and Keller and Colloca (2007) applied an excitation that consisted of a sinusoidal load with a stepwise increased frequency up to 50 Hz and calculated the ratio between the applied force and the measured deflection or velocity for each frequency band. The interest of these studies was to examine the stiffness-frequency or impedance-frequency relation in a single loading direction, since it is known that the damping component that is present in a viscoelastic structure as the spine produces a stiffening effect with increasing frequency. Kasra et al. (1992) did set out to find the resonance frequencies of human motion segments under different preloads and in different structural conditions. They found resonance frequencies between 23 and 35 Hz depending on the applied preload but found no significant change in resonance frequency after removal of the posterior elements. Kawchuk et al. (2008, 2009) studied vibration testing with assessment of the FRF in the frequency domain up to 2 kHz in multiple directions. They performed tests in cadaveric pigs before and after successive disc transection and mounting of scoliosis instrumentation and calculated the frequency response correlation coefficient to compare the FRFs of the different structural states. In their second study, they also applied a structural health monitoring system to identify the presence, location and magnitude of structural changes. Their studies showed that FRF data can be used to identify the presence, location and magnitude of structural alterations, but the authors did not determine resonance frequencies and corresponding mode shapes and were (therefore) unable to assign specific FRF features to specific alterations in structural state (e.g. linkage of L1-L2 leads to an increase in the resonance frequency for bending).

The main objective of the present study was to determine if structural vibration testing can reveal the resonance frequencies of spinal motion segments that correspond to the mode shapes flexion–extension bending, lateral bending and axial rotation. The second objective was to establish whether resonance frequencies can discriminate specific structural alterations of the motion segment.

2. Materials and methods

2.1. Specimens

Six lumbar spines from Dutch milk goats were obtained from the abattoir, wrapped in plastic bags and stored at -21 °C. Eighteen hours prior to vibration testing, the spines were thawed to room temperature and the musculature was carefully removed, leaving the ligaments intact. The spines were dissected in single motion segments resulting in 4 × T16–L1, 6 × L2–L3 and 6 × L4–L5; sixteen single motion segments in total. Three screws were inserted in the lower end vertebra, which was then embedded in a cup using a low melting temperature alloy (Wood's metal). A hole was drilled in one of the pedicles of the upper vertebra, and a screw was inserted for later shaker attachment. Saline-soaked gauze was wrapped around the specimens and sprayed with saline solution during preparation to minimise dehydration.

2.2. Vibration equipment and test setup

Vibration was provided by an electromagnetic vibration exciter (shaker, Brüel & Kjær, type 4810) suspended on springs from a tripod. The shaker was attached to the screw in the upper vertebra with use of a stinger (flexible steel rod). The applied vibration force was quantified by a piezoelectrical load cell (Brüel & Kjær, type 8203) placed in between the stinger and the screw in the specimen. The response was collected by uniaxial accelerometers (Brüel & Kjær, type 4393), each weighing 1 g, attached with bee wax to the transverse processes of the upper vertebra in anteroposterior direction and to the spinous process and the ventral side of the upper vertebra in mediolateral direction (Fig. 1).

The excitation signal was provided by a digital signal processing system (Siglab, model 20-42) that was connected to a laptop computer. The excitation signal was current driven amplified (Brüel & Kjær, type 2706) and consisted of random frequencies between 0 and 2 kHz. The applied vibration force and the response from the accelerometers were amplified (Brüel & Kjær, type NEXUS, 4-channel) and fed back to the Siglab system. The sample frequency was set at 5120 Hz. During measurements, the coherence of input and output signals (with values between 0 and 1) was available as feedback on the monitor. When the coherence was <0.8 the measurement was considered of insufficient quality and the trial was repeated. A schematic drawing of the measurement setup is provided in Fig. 2.

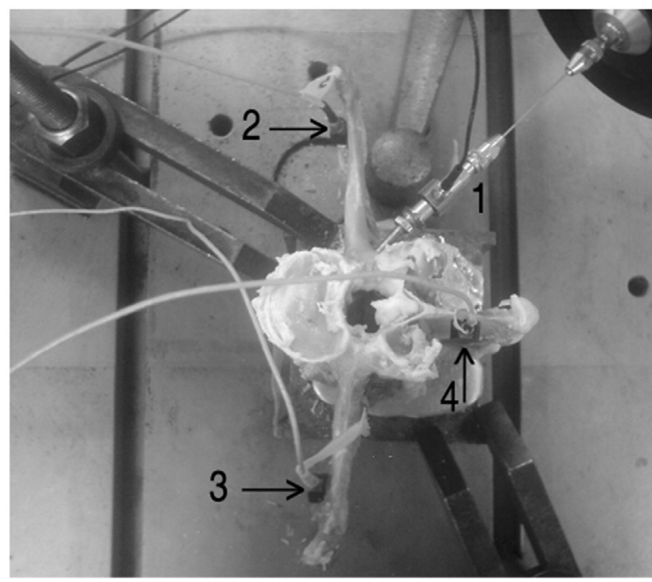

Fig. 1. Top view of the specimen with accelerometers attached to the transverse processes (2 and 3) to measure the response in anteroposterior direction and to the spinous process (4) to measure the response in mediolateral direction. The shaker (1) is attached to a screw in the pedicle.

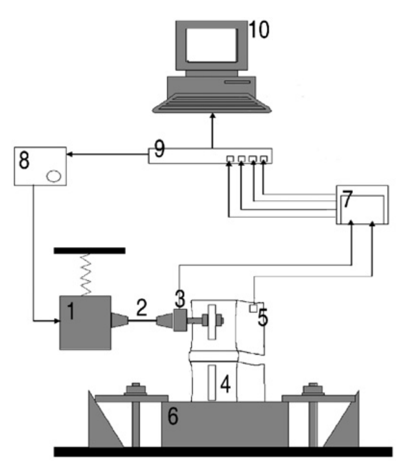

Fig. 2. Measurement setup with shaker (1), stinger (2), force transducer (3), specimen (4), accelerometer (5), cup in which the specimen was embedded (6), conditioning amplifier (7), power amplifier (8), digital signal processing system (9) and PC (10).

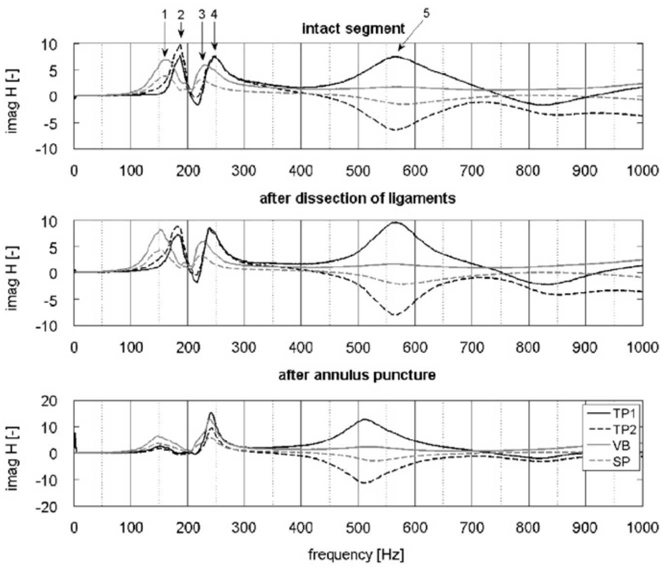

Fig. 3. Typical example of a FRF from one specimen. The imaginary part of the FRF, Im{$H(\omega)$}, is plotted versus the frequency. The four lines in the graph represent the FRFs of the two sensors on the transverse processes (TP1 and TP2): the sensor on the spinous process (SP) and the sensor on the vertebral body (VB). Clear resonance peaks indicated by the numbers 1–5 in the graph can be identified. The middle and lower panels show the FRFs after the structural condition of the segment was altered.

2.3. Experimental procedure

To examine whether alterations in the structural integrity affected the resonance frequencies, trials were performed in three different structural conditions: (1) intact, (2) after the dissection of the interspinous, supraspinous and intertransverse ligaments, ligamenta flava and the facet capsular ligaments and (3) after puncturing the annulus fibrosis at the ventral side of the intervertebral disc with a 5 mm diameter punch. To examine linearity trials were performed at two different force levels in a subset of eight segments.

2.4. Data analysis

Excitation and response data were extracted using a computer programme written in Matlab (Mathworks, Natick MA, USA). First, the cross power spectral density of the response and excitation signal $S_{XF}(\omega)$ and the power spectral density of the excitation signal $S_{FF}(\omega)$ were calculated according to Welch's averaged modified periodogram method of spectral estimation, using a Hamming window with a window size of half the sample frequency and 50% overlap. From these, the frequency response function (FRF) was calculated as the quotient of $S_{XF}(\omega)$ and $S_{FF}(\omega)$. In connection with the 90° phase criterion, the imaginary part of the FRF displays a peak when the excitation frequency is equal to the resonance frequency; therefore, the imaginary part of the FRF was plotted versus the frequency. The locations of the first five resonance peaks of the FRF were then determined for the three conditions for each specimen. Since the specimens were taken from three segmental levels, this procedure resulted in 5 (peaks) $\times$ 3 (conditions) $\times$ 3 (segmental level) $=$ 45 mean frequencies with standard deviations (Fig. 4). Phase differences between the response signals were used to characterize the type of mode shape (e.g. bending or torsion) of the resonance frequencies (Fig. 3). Linearity was checked by overlaying the two FRFs obtained from the two different excitation levels (Fig. 5).

2.5. Statistics

Statistical analysis was performed to examine whether the resonance frequencies were significantly different for the three structural conditions and for the three segmental levels, and whether segmental level and condition interacted. Because several specimens were obtained from one goat spine, observations might not be independent. Therefore, linear multilevel analysis was used, which is an extension of standard regression techniques (Twisk et al., 2006; Fields, 2009). All statistical tests were performed using SPSS 16 (SPSS Inc., Chicago, IL); significance was set at $p<0.05$.

3. Results

Fig. 3 shows a typical example of a FRF. The four lines in the graph represent the FRFs of the two sensors on the transverse processes (TP1 and TP2), the sensor on the spinous process (SP) and the sensor on the vertebral body (VB). Clear resonance peaks indicated by the numbers 1–5 in the graph could be identified in all segments. The middle and lower panels show the FRFs after the structural condition of the segment was altered. In this typical example, peaks 2, 4 and 5 appear to have shifted to the left hand side after the annulus was punctured. Fig. 4 shows the mean values and standard deviations (in Hz) for the resonance frequencies 1–5 of all 16 specimens for the three structural conditions and for the three segmental levels.

3.1. Assessment of the mode shape

Assessment of the phase information from the two accelerometers on the two transverse processes (TP1 and TP2 in Fig. 3) shows that the sensors moved in-phase at the frequencies of peaks 2 and 4 and in anti-phase at the frequency of peak 5. In-phase movement indicates that the mode shape was a bending or a shear mode and anti-phase motion indicates that the mode shape was axial rotation. The phase information from the signals from the accelerometers on the spinous process and on the ventral side of the vertebra (VB and PS in Fig. 3) shows that peaks 1 and 3 corresponded to lateral bending or lateral shear.

3.2. Building the multilevel linear model

Before the model was constructed, the parameter "condition" was recoded into two levels using dummy variables: intact versus no ligaments (I–nL) and no ligaments versus annulus puncture (nL–P). The multilevel model was built up starting with fixed parameters only (condition and segment level), after which random coefficients were added (random intercept for goat and a random slope for segment level). Improvement of the model overall fit was tested using chi-square likelihood tests comparing the old and the new models. The relationship between resonance frequencies and segment level showed significant variance in intercepts across goats, var(u_{0j})$=$354.79, $\chi^2(1)=21.46$, $p<0.01$. In addition, slopes varied across goats, var(u_{1j})$=$653.74, $\chi^2(1)=26.30$, $p<0.01$. There was no significant covariance between slopes and intercepts. The final model therefore consisted of "goat" as subject variable, with "I–nL", "nL–P", "segment level" and the interaction between "segment level" and "I–nL" and between "segment level" and "nL–P" as fixed coefficients with a random intercept and random slope for "segment level".

3.3. Statistical results of the resonance frequencies

The structural condition predicted the resonance frequency; dissection of ligaments had a borderline significant effect on the prediction of peak 1 ($F(1,26)=3.920$, $p=0.058$), and puncturing the annulus fibrosis had a highly significant effect on the prediction of the resonance frequencies for peaks 4 and 5, and almost significant for peak 2 ($F(1,26)=9.678$, $p=0.004$, $F(1,26)=78.328$, $p<0.001$ and $F(1,26)=3.075$, $p=0.091$, respectively). The segment level significantly predicted the resonance frequencies for peak 5 and a trend was observed for peak 3 ($F(2,13.63)=8.995$, $p=0.003$ and $F(2,9.411)=3.292$, $p=0.082$, respectively); pairwise comparisons showed that resonance frequencies were higher for the T16–L1 segment than for the L4–L5 and L2–L3 segments. The interactions between segment level and condition did not significantly predict the resonance frequency, which indicates that manipulating the integrity of the segment had the same effect on all the segmental levels tested.

3.4. Linearity check

All specimens exhibited linear characteristics when excited in the intact condition. After dissection of the ligaments and

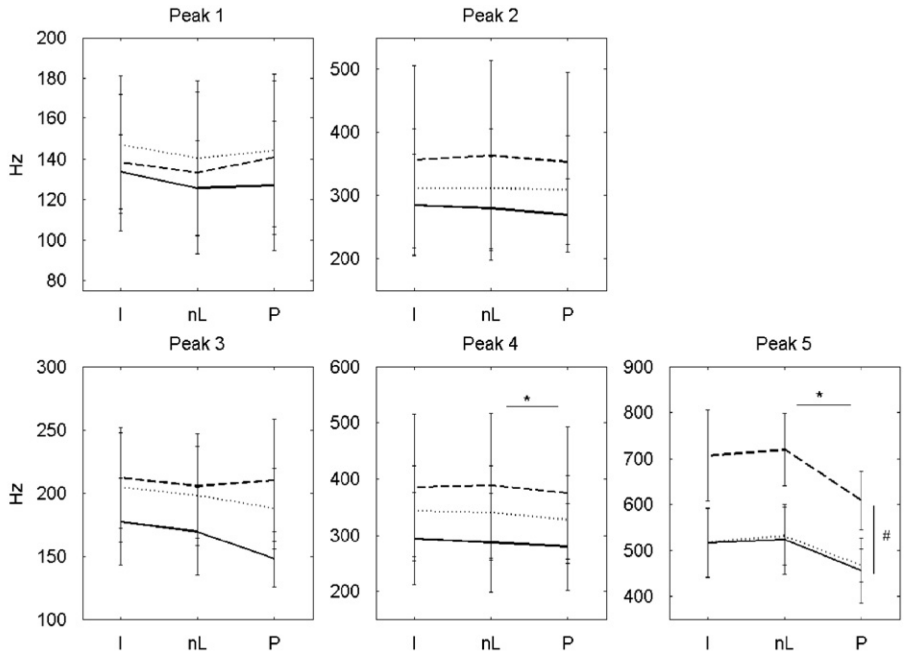

Fig. 4. Mean values and standard deviations of the frequencies of resonance peaks 1–5 for L4–L5 (solid line), L2–L3 (dotted line) and T16–L1 (dashed line) for the three conditions (I, intact; nL, no ligaments; P, after annulus puncture). The asterisks indicates a significant reduction in the resonance frequency for all segments when the annulus was punctured. The hash symbol indicates that the resonance frequency was significantly higher for T16–L1 than for L2–L3 and L4–L5 in the punctured condition.

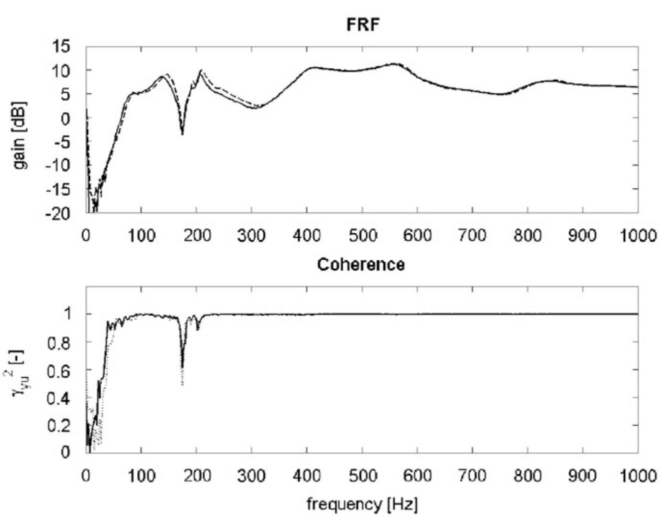

Fig. 5. Typical example of the two FRFs obtained at different force levels after dissection of the ligaments and puncturing of the anulus. A slight difference between the lines occurs between 0 and 400 Hz, suggesting that nonlinearities were excited in this frequency range. Apart from the frequencies around 200 Hz the coherence is > 0.8 in this interval; therefore loss of linearity was probably not due to measurement noise.

puncturing of the annulus only two out of eight specimens showed a slight difference between the two FRFs obtained at different force levels between 0 and 400 Hz, suggesting that nonlinearities were excited in this frequency range (Fig. 5).

4. Discussion

Structural vibration testing is a non-destructive measurement technique that is used in engineering to identify the mechanical properties of a structure and can be used to identify structural damage, such as cracks. The main objective of this study was to determine if structural vibration can reveal the resonance frequencies of spinal motion segments for flexion–extension bending, lateral bending and axial rotation. The results showed similar ''smooth'' FRF-curves with clear resonances for all segments. Clear resonance peaks indicate that the modes are sufficiently far apart to make differentiation possible and that damping is sufficiently low to make the peaks stand out of the rest of the curve. These results are in accordance with previous findings on the applicability of modal testing in biomechanical applications. Cornelissen et al. (1986, 1987) and Christensen et al. (1986) performed several studies on the stiffness of the human tibia and the use of modal parameters to monitor fracture healing and found that structural vibration testing and modal analysis might have clinical utility.

In addition to clear resonance frequencies, it was also possible to identify which peak corresponded to axial rotation; however, using phase information it was not possible to determine whether peak 2 or peak 4 corresponded to flexion–extension and whether peak 1 or peak 3 corresponded to lateroflexion. Phase information only shows that the sensors moved in-phase; however, this also happens during shear movements or during higher order bending modes; when the first bending mode is visualised as a simple arc, the second bending mode would have had the shape of a sine. Shear movement and higher bending modes would have resulted in a higher resonance frequency, making it likely that peak 1 corresponded to lateroflexion and peak 2 corresponded to flexion–extension. Another mode shape that might have corresponded to peak 3 and peak 4 might be the coupled motion of bending and torsion, which is normal motion behaviour for the lumbar spine (Barnes et al., 2009; Li et al., 2009). Additional measurements with more sensors are needed to determine the mode shape that corresponded to peaks 3 and 4.

The second objective was to establish whether resonance frequencies can discriminate specific structural alterations of the motion segment. The results show that puncturing the annulus fibrosis, which was performed to decrease the axial stiffness of the segment, indeed reduced the frequency of peak 5 that might correspond to a torsion mode. However, dissection of the ligaments did not significantly change the resonances for peaks 1 and 3 for lateroflexion and flexion–extension, respectively. A lack of effect on the FRF of ligament dissection was also found for the sacroiliac joint by Conza et al. (2007). They explained their lack of results compared to other studies by the fact that they performed dynamic tests, while the other studies performed static tests. Although they did not elaborate on the differences between static and dynamic (vibration) testing, their reasoning might be correct. In vibration testing, the amplitude of motion is typically very low; in spinal segment testing this low amplitude might imply that the segment moves within the neutral zone. Previous studies found that motions within the neutral zone implicate that the ligaments are not stretched and therefore add no stiffness to the segment (Panjabi, 1992; Crawford et al., 1998). Accordingly, removing the ligaments does not reduce the resonance frequency. Removal of the ligaments might even have increased the resonance frequencies in some cases in the present study (Fig. 3). This can be explained by the fact that removing ligamentous tissue also means that mass is removed from the system; a reduction in mass at constant stiffness increases the resonance frequency. Since the ligamentous tissue that was removed weighed around 15 g and the mass of the intact system was around 83 g, this could account for an increase in the resonance frequency by some 10%. The reduction in the resonance frequency for axial rotation after puncturing the annulus fibrosis was as expected. From engineering practise the rotational stiffness is known to be largely affected when a cylinder wall is interrupted by drilling a hole. The effect of an interruption of the annulus fibrosis on the rotational stiffness was studied recently in rat tails by Michalek et al. (2010). The authors measured rotational stiffness in intact discs and after needle puncture injuries with a 30 G, a 25 G and a 21 G needle, and found a significantly lower axial rotational motion after the annulus was punctured by a needle >25 G. However, they also found that the torsion behaviour in the neutral zone, where the annular fibres are lax, was not affected by the puncture. The contrast between the findings of Michalek et al. and the findings in the current study could mean that the response amplitude of the axial rotation was beyond the neutral zone and therefore annulus fibres did contribute to the rotational stiffness. This is not necessarily in contrast to the previous explanation that the segment did not move beyond the neutral zone, since the neutral zone is smaller in axial rotation than in flexion–extension and lateroflexion, as was found by Busscher et al. (2010) in human and porcine spines. The stiffness contribution of the annulus fibrosus may be large compared to the ligaments, because of its shorter collagen fibres and higher cross-sectional area.

5. Conclusion

This study showed that the resonance frequencies of spinal motion segments for flexion–extension, lateroflexion and axial rotation can be determined by structural vibration testing, and that resonance frequencies can discriminate specific structural alterations of the motion segment. Based on these results, vibration testing might be a promising method to study the mechanical properties of larger spinal sections and ultimately patients suffering from low back disorders.

Conflict of interest statement

There are no financial and personal relationships with other people or organisations that inappropriately biased this work and no funding was received.

Acknowledgements

The authors would like to thank Bert Wolbert from the Department of Applied Mechanics, University of Twente, Enschede, for his advice during the design of the experimental setup and the preliminary investigations.

References

Barnes, D., Stemper, B.D., Yoganandan, N., Baisden, J.L., Pintar, F.A., 2009. Normal coupling behavior between axial rotation and lateral bending in the lumbar spine. Biomedical Sciences Instrumentation 45, 131–136.
Busscher, I., Van der Veen, A.J., Van Dieën, J.H., Kingma, I., Verkerke, G.J., Veldhuizen, A.G., 2010. In vitro biomechanical characteristics of the spine: a comparison between human and porcine spinal segments. Spine 35 (2), E35–E42.
Christensen, A.B., Ammitzbøll, F., Dyrbye, C., Cornelissen, M., Cornelissen, P., Van der Perre, G., 1986. Assessment of tibial stiffness by vibration testing in situ—I. Identification of mode shapes in different supporting conditions. Journal of Biomechanics 19 (1), 53–60.
Conza, N.E., Rixen, D.J., Plomp, S., 2007. Vibration testing of a fresh-frozen human pelvis: the role of the pelvic ligaments. Journal of Biomechanics 40 (7), 1599–1605.
Cornelissen, M., Cornelissen, P., Van der Perre, G., Christensen, A.B., Ammitzboll, F., Dyrbye, C., 1987. Assessment of tibial stiffness by vibration testing in situ—III. Sensitivity of different modes and interpretation of vibration measurements. Journal of Biomechanics 20 (4), 333–342.
Cornelissen, P., Cornelissen, M., Van der Perre, G., Christensen, A.B., Ammitzbøll, F., Dyrbye, C., 1986. Assessment of tibial stiffness by vibration testing in situ—II. Influence of soft tissues, joints and fibula. Journal of Biomechanics 19 (7), 551–561.
Crawford, N.R., Peles, J.D., Dickman, C.A., 1998. The spinal lax zone and neutral zone: measurement techniques and parameter comparisons. Journal of Spinal Disorders 11 (5), 416–429.
Fields, A.P., 2009. Multilevel Linear Models: Discovering Statistics using SPSS. Sage, London.
Haughton, V.M., Lim, T.H., An, H., 1999. Intervertebral disk appearance correlated with stiffness of lumbar spinal motion segments. AJNR American Journal of Neuroradiology 20 (6), 1161–1165.
Kaigle, A., Ekström, L., Holm, S., Rostedt, M., Hansson, T., 1998. In vivo dynamic stiffness of the porcine lumbar spine exposed to cyclic loading: influence of load and degeneration. Journal of Spinal Disorders 11 (1), 65–70.
Kasra, M., Shirazi-Adl, A., Drouin, G., 1992. Dynamics of human lumbar intervertebral joints: experimental and finite-element investigations. Spine 17 (1), 93–102.
Kawchuk, G.N., Decker, C., Dolan, R., Carey, J., 2009. Structural health monitoring to detect the presence, location and magnitude of structural damage in cadaveric porcine spines. Journal of Biomechanics 42 (2), 109–115.
Kawchuk, G.N., Decker, C., Dolan, R., Fernando, N., Carey, J., 2008. The feasibility of vibration as a tool to assess spinal integrity. Journal of Biomechanics 41 (10), 2319–2323.
Kazarian, L., 1972. Dynamic response characteristics of the human vertebral column: an experimental study on human autopsy specimens. Acta Orthopeadica Scandinavia, 1–186.
Keller, T.S., Colloca, C.J., 2007. Dynamic dorsoventral stiffness assessment of the ovine lumbar spine. Journal of Biomechanics 40 (1), 191–197.
Li, G., Wang, S., Passias, P., Xia, Q., Li, G., Wood, K., 2009. Segmental in vivo vertebral motion during functional human lumbar spine activities. European Spine Journal 18 (7), 1013–1021.
Mao, G.P., Zhao, J.N., Wang, Y.R., Li, J.S., Chen, Y.X., Wu, S.J., Bao, N.R., 2005. Design of cervical pedicle locator and three-dimensional location of cervical pedicle. Spine (Phila Pa 1976) 30 (9), 1045–1050.
Michalek, A.J., Funabashi, K.L., Iatridis, J.C., 2010. Needle puncture injury of the rat intervertebral disc affects torsional and compressive biomechanics differently. European Spine Journal 19 (12), 2110–2116.
Panjabi, M.M., 1992. The stabilizing system of the spine. Part II. Neutral zone and instability hypothesis. Journal of Spinal Disorders 5 (4), 390–396 discussion 397.
Richardson, M.H., 1977. Derivation of Mass, Stiffness and Damping Parameters from Experimental Modal Data. Hewlett Packard Company, Santa Clara Division June.
Schmidt, T.A., An, H.S., Lim, T.H., Nowicki, B.H., Haughton, V.M., 1998. The stiffness of lumbar spinal motion segments with a high-intensity zone in the anulus fibrosus. Spine (Phila Pa 1976) 23 (20), 2167–2173.
Subramaniam, V., Chamberlain, R.H., Theodore, N., Baek, S., Safavi-Abbasi, S., Senoglu, M., Sonntag, V.K., Crawford, N.R., 2009. Biomechanical effects of laminoplasty versus laminectomy: stenosis and stability. Spine 34 (16), E573–E578.
Tai, C.L., Hsieh, P.H., Chen, W.P., Chen, L.H., Chen, W.J., Lai, P.L., 2008. Biomechanical comparison of lumbar spine instability between laminectomy and

bilateral laminotomy for spinal stenosis syndrome—an experimental study in porcine model. BMC Musculoskeletal Disorders 9, 84.

Twisk, J.W.R., Ellenberg, S., Elston, R., Everitt, B., Harrell, F., 2006. Applied Multilevel Analysis: A Practical Guide for Medical Researchers. Cambridge University Press, Cambridge.

Van Solinge, G.B., Van der Veen, A.J., Van Dieën, J.H., Kingma, I., Van Royen, B.J., 2010. Anterior shear strength of the porcine lumbar spine after laminectomy and partial facetectomy. European Spine Journal 19 (12), 2130–2136.

Zhao, F., Pollintine, P., Hole, B.D., Dolan, P., Adams, M.A., 2005. Discogenic origins of spinal instability. Spine (Phila Pa 1976) 30 (23), 2621–2630.